59th ILMENAU SCIENTIFIC COLLOQUIUM
Technische Universität Ilmenau, 11 – 15 September 2017
URN: urn:nbn:de:gbv:ilm1-2017iwk-070:0

Transmission Volume Holograms for LED Illumination

Daniela Karthaus[1], Oliver Sandfuchs[2], Stefan Sinzinger[3]
[1]HELLA KGaA Hueck & Co., Lippstadt, Germany
[2]University of Applied Sciences Hamm-Lippstadt, Germany
[3]Ilmenau University of Technology, Germany

ABSTRACT

The application of transmission holograms in automotive headlamp systems is a possible new field of application for holographic elements. However, it requires the adaptation of holograms to light-emitting diodes (LEDs) as reconstruction light sources. This includes the consideration of the reconstruction wavefront shape. Therefore, computer-generated holograms (CGHs) are designed for different LED wavefront approximations and recorded in a photopolymer. Within experiments, the performance of the optimization is analyzed. For reconstruction, an automotive-certified LED is used and the reconstructed image is recorded. The correlation of the ideal and the real reconstructed image is used as indicator for a successful adaptation within the design process. It is shown that there are clear differences regarding the improvement of the correlation between the considered wavefront approximations. The best results are achieved with a wavefront, determined from an interferometric measurement, and with a wavefront with Lambertian characteristic.

Index Terms - Holography, Computer-generated holograms, LED, illumination

1. INTRODUCTION

The application of transmission volume holograms as optical elements in automotive illumination systems provides advantages like low axial thickness, light weight and a high flexibility regarding the design and the functionalities. Due to multiplexing properties [1], holograms can take the function of several optical elements like lenses and apertures. Especially computer-generated holograms (CGHs) can be designed in arbitrary ways and are versatile usable. However, the design and the recording process limits the range of usable illumination light sources. To get the best quality of the reconstructed image, the holograms must be illuminated with the wavelength and the wavefront shape of the recording laser. Otherwise, the resulting image is blurred and dispersion effects occur (c.f. Ref. [2-4]). Therefore, the application in headlamp systems requires the adaptation of CGHs to the illumination with typical automotive light sources. These light sources are polychromatic and divergent, e.g. phosphor-converted white LEDs with divergence angles of about ±60°. In the literature, spectral filters and lenses are used to adapt the light of LEDs to the design parameters (c.f. Ref. [5,6]), instead of optimizing the hologram. However, the usage of additional optical components reduces the benefits of the application of holograms in automotive systems. It has already been shown that dispersion effects can be avoided by considering spectral information of the illuminating light source within the design or the recording process, e.g. for reflection holograms with RGB-illumination (c.f. Ref. [5,7]) or for holographic lenses (cf. Ref. [8]). The specific angular emission of LEDs is not considered so far or it is approximated by ideal wavefront descriptions like spherical waves [9,10]. Therefore, CGHs should be designed for the specific wavefront shape of an LED. In section 2, the computational design process for the optimization of holograms is presented,

and the different ways to approximate an LED wavefront are described in section 3. The experimental test series and their results are briefly illustrated in section 4. Finally, the results and future steps are discussed in section 5.

2. COMPUTATIONAL OPTIMIZATION OF CGHS

The objective of the hologram optimization is the minimization of the difference between the desired ideal reconstructed image I_Z and the real reconstructed image I_R. In other words, the images I_Z and I_R should be as similar as possible. The similarity can be analyzed by calculating the correlation coefficient of both images with the pixel positions (k, l) and the mean values of the images $\bar{I}_Z$ and $\bar{I}_R$, according to

$$\rho = \frac{\sum_k \sum_l \left[\left(I_R^{k,l} - \bar{I}_R\right)\left(I_Z^{k,l} - \bar{I}_Z\right)\right]}{\sqrt{\left[\sum_k \sum_l \left(I_R^{k,l} - \bar{I}_R\right)^2\right]\left[\sum_k \sum_l \left(I_Z^{k,l} - \bar{I}_Z\right)^2\right]}} \,. \tag{1}$$

The value of the coefficient can achieve values between 0 and 1, whereby 0 indicates no similarity and 1 indicates identical images. For the analysis of the experiments this means, the higher the value of ρ, the smaller is the difference between the images and the better is the optimization of the CGH for the illuminating light source.

A three-step design process is used for the optimization, which is illustrated in Fig. 1. First, a basic hologram is designed to generate a specific test pattern. This calculation is performed with the iterative Fourier transform algorithm (IFTA) [11] resulting in a phase pattern $\varphi_B(x,y)$. It is defined, that the size of the reconstructed image must be equal for an arbitrary reconstruction wavelength, differing from the recording wavelength of 532nm. This is realized by using a wavelength-dependent scaling factor for the image template (for details see Ref. [12]).

The following design step is influenced by the recording process. There are different options to record a CGH into a material, e.g. two- or multi-photon processes [13] or displaying of the holographic information with a spatial light modulator (SLM) [14,15]. The latter is used for recording the holograms presented in this paper. In general, a hologram can be recorded in one step using a SLM, as the two-dimensional phase information from the IFTA is displayed by a two-dimensional device. However, it can be necessary to build up the hologram in a multi-step process, e.g. if several viewpoints of the object are desired [16,17]. The local optimization of the holograms, as presented in this paper, requires also a multi-step process, in which the hologram is build up as a matrix of several subholograms. This provides the possibility to adapt each subhologram to the local wavefront information [18]. Therefore, the phase pattern $\varphi_B(x,y)$ is replicated to get a matrix of $M \times N$ subholograms in step two. The correct visual appearance of the test pattern requires the superposition of all reconstructed images at the same local position on a screen and, hence, an individual modification of each subhologram. This modification is comparable to the addition of the phase information of a lens $\varphi_L(x,y)$, whose focal length is corresponding to the distance between the hologram and the screen. However, the reconstruction wavelength must be considered again to avoid a blurred reconstructed image (for details, see Ref. [12]). The holographic phase information $\varphi_S(x,y)$ resulting from the second design step generates the best reconstructed image when it is illuminated with a plane wave. The adaption to an arbitrary wave is realized in step three. Therefore, the conjugate phase information $\varphi_R(x,y)$ of the local wavefront is added to the subholograms (for details, see Ref. [18]). At the end of the three-step process, $M \times N$ subholograms $\varphi_H(x,y)$ are designed for an arbitrary wavelength and wavefront. The advantage is that there are no restrictions regarding the wavefront shape in the computational design, if the 2π-modulated phase is adequately sampled. However, an important aspect is the similarity between the assumed and the real wavefront information of the reconstruction light source.

Deviations of these waves lead to a deterioration of the visual appearance of the reconstructed image. In the next section, LED wavefront approximations are presented, which have been used for hologram optimizations.

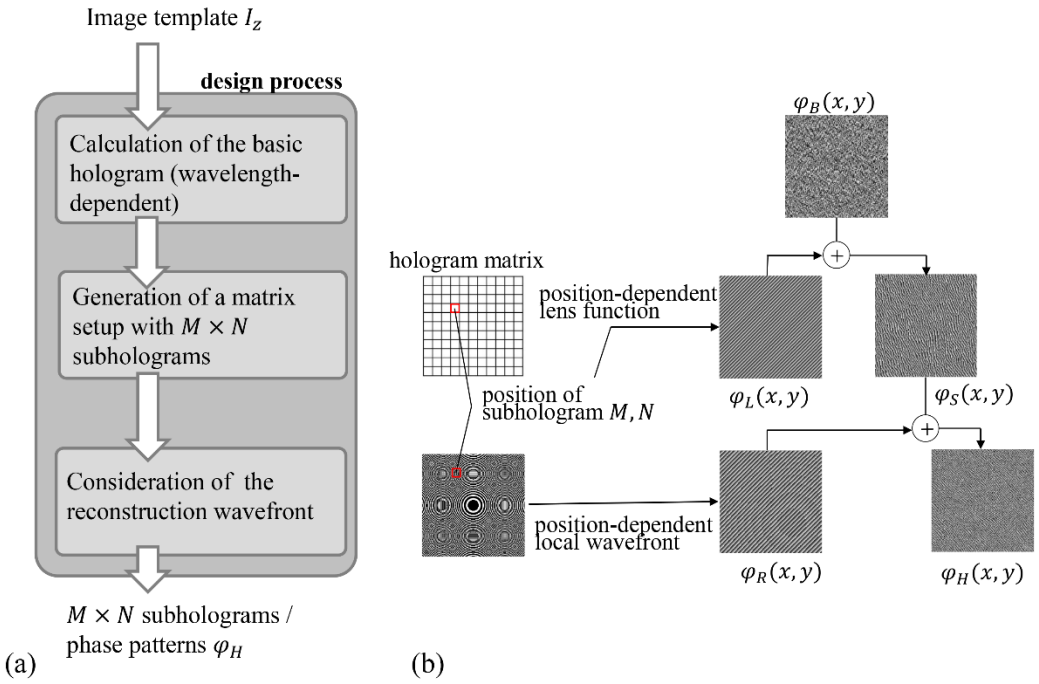

Figure 1: Schematic flowcharts of the design process. (a) the three-steps procedure in general, including the calculation of the basic hologram, the generation of the hologram matrix and the consideration of the local reconstruction wavefront; (b) same procedure as in (a) regarding the resulting phase pattern of each step.

3. APPROXIMATIONS OF LED WAVEFRONTS

There are two options to describe the emission of an LED in general. The first is the approximation as a spherical wave, due to the small chip dimensions and the highly divergent emission. Using the parabolic approximation, the phase of a spherical wave can be described as

$$\varphi_{SW}(x,y,z) = arg\left\{exp\left[-\frac{i\pi}{\lambda z_0}(x_0+x)^2+(y_0+y)^2\right]\right\}, \quad (2)$$

with λ as wavelength, i as imaginary unit number, (x,y,z) are coordinates of the observation plane and (x_0, y_0, z_0) are coordinates of the wave's source plane. However, the light emitting surface of an LED is not infinitesimally small. It is assumed, that the consideration of the surface dimension leads to better results. According to Huygens' principle [2], the LED wavefront can be constructed by superimposing a number of spherical waves, that are emitted from different local positions on the LED chip. This is a well-known approach to construct wavefronts [9,19]. The simplest mathematical formulation of Huygens' principle is the summation of $G \times H$ spherical waves according to

$$\varphi_{HP}(x,y,z) = arg\sum_{g=1}^{G}\sum_{h=1}^{H} exp\left[-\frac{i\pi}{\lambda z_0}\left(x_{gh}+x\right)^2+\left(y_{gh}+y\right)^2\right] \quad (3)$$

Another formulation that has been established, is the Rayleigh-Sommerfeld approximation (RS). This describes the diffraction of waves at an aperture by superposing spherical waves

located in the aperture plane. In this paper, the convolution-based formulation of the RS approximation is used according to [20]

$$\varphi_{RS}(x,y,z) = arg\left[\mathcal{F}^{-1}\{\mathcal{F}\{U(x_0,y_0,z_0)\}\mathcal{F}\{H(x,y,z)\}\}\right] \quad (4)$$

$$\text{with} \qquad \mathcal{F}\{H(x,y,z)\} = \exp\left[\mathrm{i}2\pi\sqrt{\frac{1}{\lambda^2} - f_x^2 - f_y^2}\right].$$

In these equations, (f_x, f_y) are the spatial frequency coordinates in the Fourier Domain, $\mathcal{F}$ is the operator of the Fourier transform and $\mathcal{F}^{-1}$ the operator of the inverse Fourier transform.
The presented approaches allow the consideration of the LED dimension, which is generally provided by LED manufacturers. However, these approaches are limited with regard to effects of optical or material properties of phosphor-converted white light LEDs or diodes with integrated lenses. To consider these effects, an interferometry-based approach was developed to measure the emitted wavefronts of LEDs [18]. Therefore, a Mach-Zehnder interferometer is used to generate a spherical reference wave that interferes with the unmodified sample wave of the LED. A phase retrieval approach is used to extract the LED phase information from two phase-shifted interference images by a combination of different methods like the Gram-Schmidt orthonormalization method [21], the continuous wavelet transform [22] and the successive over-relaxation method [23]. For details about the wavefront reconstruction from several measurements see Ref. [18].
This interferometry-based approach provides the possibility to measure a wavefront "as is", including any influences from the chip, the package, materials or optical components. However, the approach shows a high metrological and computational effort. In addition, the interferometer setup leads to restrictions regarding the measurable wavefront region. The path lengths are 205mm. This limits the measuring to an angular region of ±0.8°. The region can be extended by rotating the LED, which leads to an angular region of ±2°, which corresponds to the size of a hologram of 13.75 x 13.75mm² (11x11 subholograms). However, this requires the recording and processing of 56 interference images [18]. In consequence, the measuring of typical emission angles of ±60° would take several weeks with the current approach.
An alternative approach to get the wavefront information of large angular regions might be the derivation from available photometric data. Manufacturer provide luminous intensity distribution curves (LDCs) for LEDs, which describe the envelope of all emitted light rays. Regarding the theory of the normal congruence between rays and waves, the wavefronts could be derived from ray files or from the luminous intensity distribution. Within the experiments presented in this paper, an automotive-certified LED (Luxeon F, Philips) is used, which has a Lambertian emission characteristic as shown in Fig. 2. The LDC has been fitted and used for additional wavefront approximation.

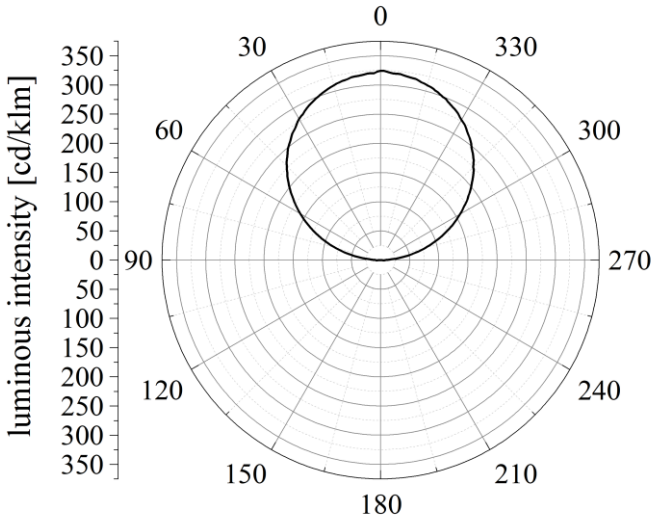

Figure 2: Luminous intensity distribution curve (LDC) of the Luxeon LED in polar coordinates. The distribution shows a Lambertian emission characteristic.

In the next section, the experimental test series to examine the effectiveness of the hologram optimization for the presented wavefront approximations are presented.

4. EXPERIMENTAL TEST SERIES AND RESULTS

The optimization of transmission holograms for LED illumination has been investigated within two test series. Therefore, holograms are designed for the different wavefront approximations and recorded into a photopolymer with the SLM-based exposure process. For the analysis of the reconstructions, the holograms are designed to generate the test pattern that is shown in Fig. 3. Within the test series, the holograms are illuminated at reference angle and the reconstructed image is projected on a semitransparent screen in the distance of 300mm behind the hologram. This image is recorded with a luminance camera, which is positioned on the optical axis 350mm behind the screen, as shown in Fig. 3. The recorded pictures are used to calculate the correlation coefficient according to Eq. 1.

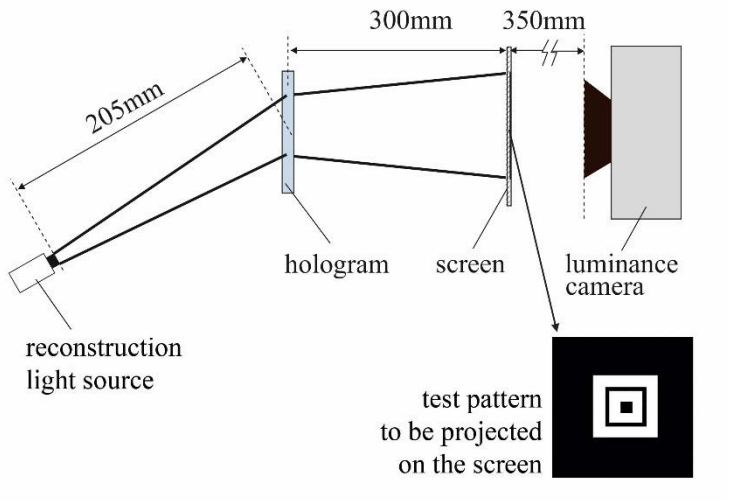

Figure 3: Schematic image of the experimental setup. The hologram is reconstructed by one of the laser diodes or the LED, which is positioned 205mm in front of the hologram. The reconstructed image should comply with the test pattern and is projected on.

In the first experimental series, the influence of the different wavefront approximations is analyzed for the wavelength 532nm, 590nm and 620nm. Four holograms are designed for the approximations spherical wave (Eq. 2), RS (Eq. 4), Huygens (Eq. 3) and for the measured wave. These holograms are illuminated with the Luxeon LED, that is filtered by appropriate color filters. In addition, one hologram is designed for a plane wave at 532nm and is reconstructed with a collimated laser diode at this wavelength. This ideal reconstruction condition is assumed to result in the maximum experimentally achievable value for the correlation coefficient, which is $\rho=0.8631\pm0.0066$.

The results have already been presented in [18] and show that the measured wave approximation leads to the best values for the correlation coefficient for all wavelengths, close to the values of the spherical wave approximation. The RS and the Huygens approximation lead to clearly lower values. For 532nm, the results are illustrated in Fig. 4. The values of the correlation coefficient for the different wavefront approximations are $\rho_{MW}=0.7663\pm0.0059$ for the measured wave, $\rho_{SW}=0.7649\pm0.0074$ for 5the spherical wave, $\rho_{HP}=0.7082\pm0.0046$ for the Huygens approximation and $\rho_{RS}=0.5930\pm0.0018$ for the RS approximation. The uncertainties result from mismatching of the reconstructed and the ideal image of ±2 pixels in x- and y-direction.

The results show, on the one hand, that neither the spherical wave nor the measured wave can be identified as the better one for the LED description. However, the repetition of these tests implies the same tendencies for the approximations for all three wavelengths [18,24]. On the

other hand, the results show that the spherical wave description leads to better results than the RS and the Huygens approximation. This is an unexpected effect, because the latter were assumed to describe the LED in a more realistic way.

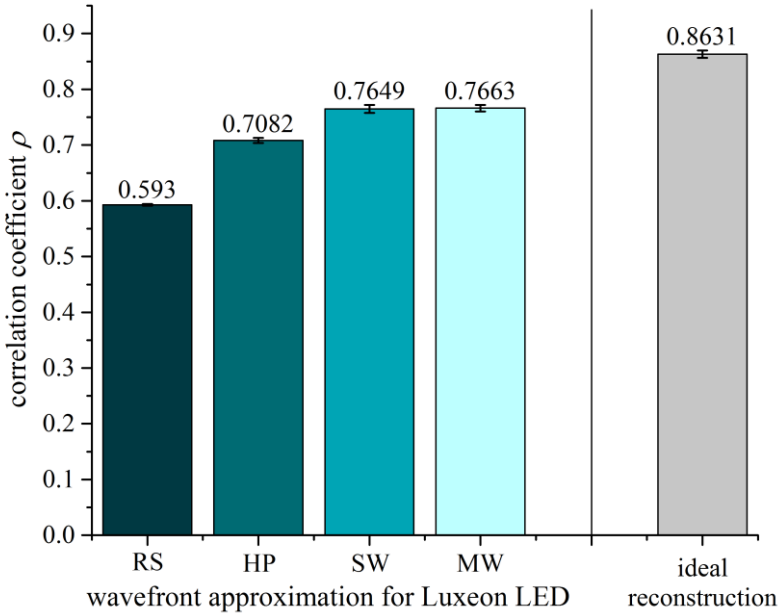

Figure 4: Correlation coefficient for the reconstructed images of the holograms optimized with different wavefront approximations at 532nm (RS=Rayleigh-Sommerfeld, HP=Huygens' principle, SW=spherical wave and MW=measured wave). Additionally, the coefficient for the ideal reconstruction is plotted (design and reconstruction with a plane wave at 532nm).

However, the analysis of the wavefront curvatures show, that the RS- and the Huygens approximation have weaker curvatures compared to the spherical and the measured wave. The supposed cause is the negligence of effects like reflection and scattering in the phosphor of the Luxeon LED, which is assumed to lead to the Lambertian emission characteristic as shown in Fig. 2. In consequence, the appropriateness of a Lambertian characteristic to describe the Luxeon LED is examined in test series two. Therefore, three holograms are designed for the spherical wave and the Lambertian characteristic for the wavelengths 532nm, 590nm and 620nm and the holograms are illuminated again with the filtered LED. For the spherical wave, the values are ρ_{SW}=0.6636±0.0087 for 532nm, ρ_{SW}=0.6715±0.0059 for 590nm and ρ_{SW}=0.6432±0.0062 for 620nm, as presented in Fig. 5.
The results show for all wavelengths higher coefficient values for the Lambertian characteristic, which reaches ρ_{LC}=0.6653±0.0080 at 532nm, ρ_{LC}=0.6868±0.0075 at 590nm and ρ_{LC}=0.6588±0.0061 at 620nm. Regarding the wavefront curvatures, a Lambertian wave shows a stronger curvature than a spherical wave. Thus, the results are reasonable, but must be verified in an outstanding repetition of this test series.
The difference of the absolute values for the spherical wave in test series two compared to test series one is supposed to be caused by straylight in the experiments. This has no influence on the comparison of the deviations between the spherical and the Lambertian wave, however, a comparison with results of the first test series is not feasible.

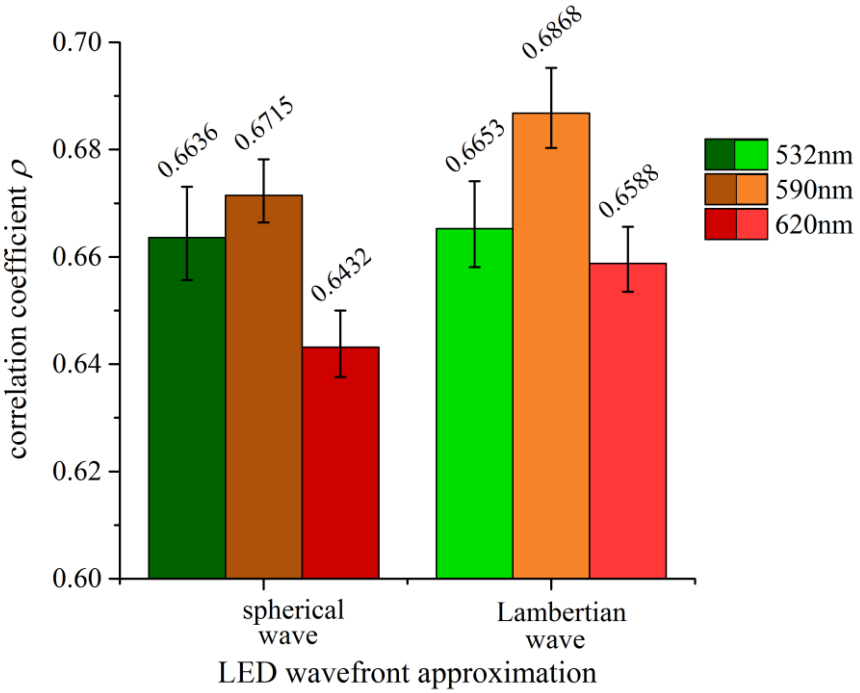

Figure 5: Correlation coefficient for the reconstructed images of the holograms optimized with a spherical and a Lambertian approximation at 532nm, 590nm and 620nm.

5. SUMMARY AND OUTLOOK

The optimization of transmission holograms for LED illumination has been investigated within two test series and the appropriateness of wavefront approximation for LEDs has been analyzed. Therefore, holograms were designed for five different wavefront approximations and the correlation between the ideal and the experimentally reconstructed images of the holograms was calculated.

It has been shown, that the approximation by an ideal spherical wave leads to higher values than the RS and the Huygens approximation. Furthermore, the measured wave and the Lambertian approximation lead to higher values compared to the spherical wave. The differences between the latter three approaches are not very high, but the tendency for an increase of the correlation coefficient for the measured wave and the Lambertian approximation has been shown for all considered wavelengths. However, further test series including greater divergence angles of the waves are necessary to clearly identify the most appropriate approximation. It is assumed, that differences between the approaches become clearer for emission angles larger than the currently measurable angular section of about ±2 degree. In addition, further experiments should address the validity of the normal congruence theory for LEDs.

REFERENCES

[1] Y. N. Denisyuk, “Thick-layered dichromated gelatin for 3d hologram multiplexing”, in Proc. SPIE 3137, Photorefractive Fiber and Crystal Devices: Materials, Optical Properties, and Applications III, pp. 216–221, 1997

[2] M. Born, E. Wolf, and A.B. Bhatia, Priciple of optics: Electromagnetic theory of propagation, interference and diffraction of light, Cambridge Univ. Press, Cambridge, 2016

[3] E. G. Loewen, and E. Popov, Diffraction gratings and applications. Marcel Dekker Inc., New York and Basel and Hong Kong, 1997

[4] G. K. Ackermann and J. Eichler, Holography: A Practical Approach, Wiley-VCH, Weinheim, 2007

[5] T. Kozacki, M. Chlipala, W. Zaperty, and P. Makowski, "Color reconstructions of real digital holograms in holographic display with white light led illumination", in Imaging and Applied Optics, OSA technical digest (online), Optical Society of America, p. DM4E.5., 2016

[6] F. Yaraş, H. Kang, and L. Onural, "Real-time phase-only color holographic video display system using led illumination". Applied Optics, 48(34), pp. H48–H53, 2009

[7] H. I. Bjelkhagen, and D. Brotherton-Ratcliffe, Ultra-realistic imaging: Advanced techniques in analogue and digital colour holography, CRC Press, Boca Raton, 2013

[8] M. Assenheimer, Y. Amitai, and A. A. Friesem, "Recursive design for an efficient hoe with different recording and readout wavelengths", Applied Optics, 27(22), pp. 4747-4752, 1988

[9] F. Wyrowski, H. Schimmel, M. Kuhn, "Elektromagnetisches Optikrechnen-Modellierung realer Lichtquellen," Photonik 39(2), 66–70, 2007

[10] T. Kari, J. Gadegaard, T. Sondergaard, T. G. Pedersen, K. Pedersen, "Reliability of point source approximations in compact LED lens designs", Opt. Express 19(6), A1190-A1195, 2011

[11] F. Wyrowski and O. Bryngdahl, "Iterative Fourier-transform algorithm applied to computer holography", JOSA A 5-7, pp. 1058–1065, 1988

[12] D. Karthaus, O. Sandfuchs und S. Sinzinger, "Design and Simulation of Computer-Generated Volume Holograms for Automotive Headlamps", in DGaO Proceedings (online), DGaO 117. Jahrestagung, Hannover, 2016

[13] E. N. Kamau, V. V. Parsi Sreenivas, M. Bülters, C. Falldorf, and R. B. Bergmann. „Fabrication of multiplexed computer-generated volume holograms in photosensitive glass", in Frontiers in Optics 2014, OSA Technical Digest (online), Optical Society of America, p. FTh4G.2. Optical Society of America, 2014

[14] C. Kohler, X. Schwab, and W. Osten, "Optimally tuned spatial light modulators for digital holography", Applied Optics, 45(5):960–967, 2006

[15] B. Li, D.-Y. Wang, Y.-X. Wang, and L. Rong, "High-resolution digital holographic imaging by using a spatial light modulator", in Proc. SPIE 9282, 7th International Symposium on Advanced Optical Manufacturing and Testing Technologies: Optical Test and Measurement Technology and Equipment, pp. 92820N0-92820N6, 2014

[16] W. Nishii and K. Matsushima, "A wavefront printer using phase-only spatial light modulator for producing computer-generated volume holograms", in Proc. SPIE 9006, Practical Holography XXVIII: Materials and Applications, pp. 9006:90061F0–90061F8, 2014

[17] S. Jolly and V. M. Bove, “Direct optical fringe writing of diffraction specific coherent panoramagrams in photorefractive polymer for updatable three-dimensional holographic display”, Journal of Physics: Conference Series 415:012054, 2013

[18] D. Karthaus, M. Giehl, O. Sandfuchs, S. Sinzinger, “Modeling of light-emitting diode wavefronts for the optimization of transmission holograms,” Appl. Opt. 56(18), 5234-5241, 2017

[19] A. Büttner, “Wave optical analysis of light-emitting diode beam shaping using microlens arrays”, Opt. Eng. 41 , 2393 – 2401, 2002

[20] F. Shen and A. Wang, “Fast-Fourier-transform based numerical integration method for the Rayleigh – Sommerfeld diffraction formula“, Appl. Opt. 45 , 1102 – 1110, 2006

[21] J. Vargas, J. A. Quiroga, C. O. S. Sorzano, J.C. Estrada, and J. M. Carazo, “Two-step demodulation based on the gram-schmidt orthonormalization method”. Optics letters, 37(3), pp. 443–445, 2012

[22] J. Ma, Z. Wang, M. Vo, and L. Luu, “Parameter discretization in two-dimensional continuous wavelet transform for fast fringe pattern analysis”. Applied optics, 50(34), pp. 6399–6408, 2011

[23] Y. Guo, X. Chen, and T. Zhang, “Robust phase unwrapping algorithm based on least squares”, Optics and Lasers in Engineering, 63, pp. 25–29, 2014

[24] D. Karthaus, M. Giehl, O. Sandfuchs and S. Sinzinger, “Optimization of Computer-Generated Transmission Holograms Using Different LED Wavefront Approximations”, in DGaO Proceedings (online), DGaO 118. Jahrestagung, Dresden, 2017

CONTACTS

M. Sc. D. Karthaus — Daniela.Karthaus@hella.com
Prof. Dr. Oliver Sandfuchs — Oliver.Sandfuchs@hshl.de
Prof. Dr. rer. nat. habil. S. Sinzinger — Stefan.Sinzinger@tu-ilmenau.de